https://doi.org/10.5194/egusphere-2026-1839
Preprint. Discussion started: 7 September 2026

The Dominance and Future Variations of Background Ozone in China under Different Climate and Emission Scenarios

Mengyun Li[1,2], Yang Yang[1,2*], Pinya Wang[2], Ke Li[1,2], Hong Liao[1,2]

[1]State Key Laboratory of Climate System Prediction and Risk Management/Jiangsu Key Laboratory of Atmospheric Environment Monitoring and Pollution Control/Jiangsu Collaborative Innovation Center of Atmospheric Environment and Equipment Technology/Joint International Research Laboratory of Climate and Environment Change, Nanjing University of Information Science and Technology, Nanjing, Jiangsu, China

[2]School of Environmental Science and Engineering, Nanjing University of Information Science and Technology, Nanjing, Jiangsu, China

*Correspondence to yang.yang@nuist.edu.cn

https://doi.org/10.5194/egusphere-2026-1839
Preprint. Discussion started: 7 September 2026

Abstract

Background ozone, defined as ozone present in the absence of domestic anthropogenic emissions, has become increasingly dominant of the total surface ozone in China as the domestic emissions decline. Using the GEOS-Chem model driven by meteorological fields from GCAP2.0, this study investigates the changes in China background ozone (CBO) from the present-day (PD) to the middle of the 21st century (MC) under the SSP1-1.9 and SSP5-8.5 scenarios. CBO consistently dominates the total surface ozone in China (CTO), accounting for about 90% of the annual mean ozone in both PD and MC conditions. Under SSP1-1.9, CTO declines by 4.7 ppbv from PD to MC, with CBO contributing 3.7 ppbv (79%) of this reduction. The decrease in CBO is largely due to a sharp decline in transboundary transport of foreign pollution ozone (FPO, –4.7 ppbv) resulting from global emission reductions, partially offset by a climate-driven increase in natural background ozone (NBO, +1.0 ppbv). Under SSP5-8.5, the annual mean CTO increases by 7.3 ppbv, of which 6.5 ppbv is attributed to the rise in CBO. The increase is primarily driven by the enhancement of NBO, associated with intensified photochemical production under warmer conditions. We also show that in a low-emission future with controlled warming, the reduction in CBO strengthens climate mitigation and creates a positive climate-ozone feedback, along with health co-benefits. These contrasting trajectories reveal that background ozone is a dynamic component shaped by global cooperation and climate change, a reality that must be considered when setting air quality targets.

https://doi.org/10.5194/egusphere-2026-1839
Preprint. Discussion started: 7 September 2026

1. Introduction

Tropospheric ozone, primarily formed through the photochemical oxidation of volatile organic compounds (VOCs) and carbon monoxide (CO) in the presence of nitrogen oxides (NO_x=NO+NO_2) under solar radiation, is a critical air pollutant with significant implications for both regional and global air quality (Yin et al., 2021; Vazquez Santiago et al., 2024; Zhou et al., 2025; Ni et al., 2026). It is also detrimental to human health and ecosystems (Emberson, 2020; Wang et al., 2023), and plays a pivotal role in atmospheric oxidizing capacity and climate dynamics (Ainsworth et al., 2012; Ma et al., 2016; Lyu et al., 2023). The prevention or control of ozone pollution has remained a significant challenge in China due to the complex photochemical processes and the varying sources of ozone precursors (Ding et al., 2019; Chen et al., 2023; Wang et al., 2025).

Background ozone, defined as ozone present in the absence of domestic anthropogenic emissions, includes contributions from both natural source precursor emissions (e.g., soil NO_x, lightning NO_x, and biogenic VOCs) and transboundary transport (Jaffe et al., 2003, 2018; Yan et al., 2021). It is also defined as the Policy-Relevant Background ozone, representing the portion of ozone that cannot be reduced under current policy frameworks, and thus provides a baseline for assessing the realistic potential of ozone mitigation (Wang et al., 2009). Studies indicated that the increasing trend of background ozone had exacerbated the frequency and intensity of high-ozone episodes in China, posing a growing challenge for effective air pollution mitigation (Chen et al., 2023). Long-term and effective ozone pollution management must consider not only local precursor emissions but also the growing influence of transboundary transport and climate-sensitive natural sources, reflecting the central importance of background ozone for developing air quality and climate policies that are both effective and adaptable to a changing climate. Given the persistent challenge of ozone pollution in China and its direct implications for public health and ecosystem sustainability, understanding the evolution of background ozone in this region is a matter of pressing policy relevance.

Several studies have recognized the critical role of background ozone and have

https://doi.org/10.5194/egusphere-2026-1839
Preprint. Discussion started: 7 September 2026

undertaken quantitative assessments of its source-specific contributions. Ni et al. (2018) quantified the contribution of transboundary transport to near-surface ozone in China using the GEOS-Chem model and showed that foreign anthropogenic emissions contributed 2–11 ppbv (parts per billion by volume) to ozone concentrations during spring. Meanwhile, Ye et al. (2024) examined the role climate-sensitive natural sources in ozone formation, finding that lightning NO_x, soil NO_x, and biogenic VOCs contribute summertime background ozone in China by 8.1, 6.4, and 3.9 ppbv, respectively. The increasing dominance of background ozone under climate change, amplified by regional transport and climate-sensitive natural sources, may offset the deficits achieved through local emission mitigation efforts (Turnock et al., 2019; Skipper et al., 2021). Given the growing influence of background ozone in shaping surface ozone concentrations, particularly as domestic anthropogenic emissions decline, it is crucial to understand how emissions and climate change shape background ozone levels.

To effectively address future risks of ozone pollution to human health and ecosystems, it is essential to understand how ozone concentrations are likely to evolve and what factors will govern those changes under different climate and emission scenarios. The Shared Socioeconomic Pathways (SSPs) describe plausible future evolutions of societal and environmental systems, detailing assumptions on population, economy, technology, and environmental development (O'Neill et al., 2014; Riahi et al., 2017). While local emission reductions are expected to lower ozone levels, studies suggest that surface ozone may still exceed health standards due to increasing background contributions. Using the GEOS-Chem model, Xu et al. (2024) found that the maximum daily 8-hour average ozone in major polluted and agricultural regions of China would surpass the WHO guideline of 100 μg m³ under most SSPs emissions scenarios by 2050. Wang and Liao (2022) emphasized the role of transboundary transport based on GEOS-Chem simulations, noting that emissions from South and Southeast Asia contributed substantially to ozone levels in China, and such impacts could be mitigated under low-emission scenarios (e.g., SSP1-1.9). Using the Community Earth System Model with an ozone tagging method, Hou et al. (2023) projected that biogenic sources could contribute up to 40% of summer surface ozone

https://doi.org/10.5194/egusphere-2026-1839
Preprint. Discussion started: 7 September 2026

concentrations over eastern China under a net-zero scenario, reflecting the growing role of natural emissions in shaping future ozone pollution patterns. These studies indicate that background ozone, driven by natural emissions and regional transport, is becoming an increasingly important factor in determining ozone pollution levels in a warmer climate.

While most previous research has focused on anthropogenic emission related-changing ozone concentrations, often overlooking the distinct evolution of background ozone. By using the chemical transport model GEOS-Chem, we investigate the temporal and spatial evolution of background ozone over China and its underlying drivers in present-day and middle of the 21st century under two diverse future scenarios, SSP1-1.9 and SSP5-8.5. Decomposing background ozone into natural and foreign-pollution components highlights how the interaction between global emission reductions and climate warming shapes the baseline that local policies must address. This understanding is crucial for informing the development of robust, climate-resilient environmental policies in China, with implications that extend to public health and climate feedbacks.

2. Data and methods

2.1 Model Description and Meteorological Inputs

The chemical transport model GEOS-Chem version 14.2.3 is employed to simulate present-day ozone concentrations and project future ozone over China. As a global three-dimensional atmospheric chemistry model, it integrates a detailed mechanism of tropospheric ozone-NO_x-hydrocarbon chemistry mechanism (Bey et al., 2001; David et al., 2019) and has been extensively applied in studies of atmospheric composition (Colombi et al., 2015; Li et al., 2020; Hu et al., 2024). The chemical mechanism incorporates hundreds of species and reactions, enabling realistic simulation of ozone formation and removal processes under varying environmental conditions. To simulate the interaction between stratospheric and tropospheric ozone, the model utilizes the linearized ozone parameterization (Mclinden et al., 2000). The model also integrates an advanced diagnostic system that quantifies the contributions

https://doi.org/10.5194/egusphere-2026-1839
Preprint. Discussion started: 7 September 2026

of chemical and physical processes, such as net chemical production, vertical convective transport, horizontal advection, dry deposition and diffusion, to ozone concentrations. Radiative forcing is quantified using the coupled radiative transfer module, the Rapid Radiative Transfer Model. Simulations from GEOS-Chem have been extensively evaluated using satellite, aircraft, and ground-based observations, and successfully applied in numerous regional and global studies related to tropospheric ozone (Shah et al., 2024; Wang et al., 2025; Zhai et al., 2024).

Meteorological inputs for the GEOS-Chem simulations in this study are provided by the Global Change and Air Pollution version 2.0 (GCAP 2.0) framework, which supplies meteorological fields under various CMIP6 (Coupled Model Intercomparison Projection Phase 6) climate scenarios across past, present, and future periods. More detailed information on GCAP 2.0 can be found in Murray et al. (2021). GCAP 2.0 provides representative time slices, including pre-industrial (1851–1860), present-day (2001–2014), mid-century (2040–2049), and end-of-century (2090–2099), which are generated under the historical condition and multiple future SSPs scenarios. The meteorological fields include key atmospheric variables such as temperature, wind components, humidity, and precipitation, which are provided at a horizontal resolution of 2° latitude × 2.5° longitude with an hourly temporal frequency. These datasets have been widely applied in studies of climate-chemistry interactions and scenario-based air quality assessments (Kang et al., 2025; Zhao et al., 2024; Murray et al., 2024). The GCAP 2.0 data during the present-day period (2011–2014, PD) and the mid-century period (2046–2049, MC) under SSP1-1.9 and SSP5-8.5 are applied in this study to represent current and projected future atmospheric conditions, respectively. SSP1-1.9 represents a sustainability-oriented pathway with aggressive mitigation measures and a target radiative forcing of 1.9 W m^{-2} by 2100, while SSP5-8.5 reflects a fossil-fueled development trajectory with weak environmental regulation and a high radiative forcing of 8.5 W m^{-2}.

2.2 Emission and Boundary Conditions

Anthropogenic emissions used in the study are derived from the CMIP6 framework. The emissions inventory includes monthly data of aerosols, and ozone

https://doi.org/10.5194/egusphere-2026-1839
Preprint. Discussion started: 7 September 2026

precursors (e.g., NO_x, CO, and VOCs), provided at a spatial resolution of 0.5°, and has been preprocessed for compatibility with the GEOS-Chem model (http://atmos.earth.rochester.edu/input/gc/ExtData). Historical anthropogenic emissions are sourced from the Community Emissions Data System (CEDS), while future emissions follow SSPs scenarios developed by integrated assessment models. Surface boundary conditions for long-lived species, such as methane (CH_4) and nitrous oxide, are prescribed as global mean surface volume mixing ratios using historical reconstructions from Meinshausen et al. (2017) and future concentrations defined under the SSPs framework (Riahi et al., 2017).

GEOS-Chem accounts for a range of natural emission sources, some of which are calculated online within the model. Lightning NO_x emissions are parameterized following Murray et al. and Ott et al. (2010) based on convective cloud-top height and flash rates. Soil NO_x emissions are computed based on the scheme by Hudman et al. (2012), which are sensitive to surface temperature, soil moisture, cloud cover, wind speed, and radiation. Biogenic VOCs emissions are computed by the Model of Emission of Gases and Aerosols from Nature (MEGAN v2.1; Guenther et al., 2012), with fluxes dynamically varying according to photosynthetically active radiation, surface temperature, and soil moisture. These climate-sensitive natural emission processes provide important background sources of ozone precursors and are included consistently across all simulation scenarios.

2.3 Experimental Design

To investigate the spatial and temporal variability of background ozone over China and to quantify the relative contributions of natural sources and transboundary transport, we conduct a series of GEOS-Chem simulations. The baseline series of simulations (BASE) adopt the above emission and meteorological settings for both PD (2011–2014) and MC (2046–2049) periods following the SSP1-1.9 and SSP5-8.5 pathways. The resulting ozone concentrations over China are referred to as total ozone (CTO). To isolate the contribution of background ozone, a set of sensitivity simulations (NO_CHN) is conducted, in which anthropogenic emissions of ozone precursors from China, including NO_x, CO, and NMVOCs, are excluded in the simulations. The resulting ozone

https://doi.org/10.5194/egusphere-2026-1839
Preprint. Discussion started: 7 September 2026

concentrations, driven exclusively by natural sources and the transboundary transport of ozone or its precursors from sources outside China, are referred to as China background ozone (CBO). A set of global sensitivity simulations (NO_ANT) is also conducted, in which all anthropogenic emissions of ozone precursors are turned off worldwide. The resulting ozone concentrations represent the natural background ozone (NBO). A summary of simulations is provided in Table 1.

The difference between CTO and CBO represents the net impact of domestic anthropogenic emissions, which is defined as China pollution ozone (CPO). Likewise, the difference between the CBO and the NBO reflects the contribution from sources outside China and is referred to as foreign pollution ozone (FPO). Based on this modeling configuration, surface ozone concentrations in the simulations can be approximately decomposed according to the following relationship:

$$CTO = CBO + CPO,\ CBO = NBO + FPO.$$

Simulations are conducted on a horizontal grid of 2° latitude × 2.5° longitude resolution and 40 vertical layers extending from the surface to 0.1 hPa. While the relatively coarse resolution limits the ability of the model to resolve urban-scale chemical gradients, it is appropriate for examining large-scale background ozone patterns across China. To ensure the stability and reliability of the simulated ozone responses to changes in climate and natural emissions, all GEOS-Chem simulations are conducted over a four-year period, preceded by an 18-month spin-up to minimize the influence of initial conditions.

3. Model evaluation

Figure. 1 compares the spatial distribution of seasonal mean surface ozone concentrations from China National Environmental Monitoring Center (CNEMC) and GEOS-Chem simulations in 2014. CNEMC provides air quality monitoring data since 2013 and this study selects 2014 as the baseline year for model evaluation, as CNEMC provides much more data in 2014 than 2013 and the historical GCAP 2.0 meteorological data ends in 2014. The model successfully reproduces the observed seasonal variation of ozone that peaks in summer and reaches their lowest levels in winter. It also captures

https://doi.org/10.5194/egusphere-2026-1839
Preprint. Discussion started: 7 September 2026

the spatial variability across China, with correlation coefficients ranging from 0.30 to 0.69 ($p < 0.01$ for all seasons). The normalized mean bias (NMB) analysis reveals consistent positive biases across all seasons, with NMB values of +23%, +16%, +19%, and +17% in winter, spring, summer, and autumn, respectively, indicating a model tendency to overestimate surface ozone concentrations. The bias is consistent with previous studies using GEOS-Chem over China and is likely attributable to uncertainties in anthropogenic emission inventories, incomplete chemical mechanisms, and the model's limited spatial resolution (Gong and Liao, 2019; Lu et al., 2019; Yang et al., 2022). Nevertheless, the model remains robust for capturing large-scale spatial and seasonal ozone patterns.

Given the limited availability of long-term surface ozone observations in China, satellite retrievals of tropospheric column ozone (TCO), obtained by combining data from the Aura Ozone Monitoring Instrument (OMI) and the Microwave Limb Sounder (MLS), serve as an important complement for evaluating model performance (https://acd-ext.gsfc.nasa.gov/Data_services/cloud_slice/new_data.html). Figure. 2 compares the annual mean TCO from the GEOS-Chem BASE simulation with satellite retrievals from OMI/MLS during 2011–2014. The model successfully reproduces the overall spatial distribution of observed TCO, including the characteristic west-to-east gradient, but slightly overestimates values, especially in regions with high pollution. Over eastern China (east of 100°E), the observed mean TCO is 40.9 DU, while the model simulates a higher value of 43.2 DU. In western China (west of 100°E), the observed and simulated values are 34.3 DU and 35.1 DU, respectively.

While some discrepancies between model simulations and observations are evident due to spatial resolution limitations, emission inventory uncertainties, and simplified chemistry, the biases remain within an acceptable range. Despite a general tendency of GEOS-Chem to overestimate both surface and tropospheric ozone, the model reproduces key spatiotemporal patterns. The comprehensive validation against multiple observational datasets underscores the credibility of the GEOS-Chem model and justifies its application in subsequent diagnostic and attribution analysis.

https://doi.org/10.5194/egusphere-2026-1839
Preprint. Discussion started: 7 September 2026

4. Background ozone from present-day to the mid-21st century

To establish a baseline for future scenario analysis, the spatial distribution of annual mean background ozone over China under the PD condition is firstly shown in Fig. 3. Spatially, CBO exhibits a distinct west-to-east decreasing gradient, with concentrations higher than 50 ppbv in western China and lower than 30 ppbv over the North China Plain (NCP) in eastern China. The simulated background ozone concentrations in this study were evaluated against available data from the literature (Chen et al., 2025, Fig. S1 and Tab. S1). The favorable regional comparison confirms the reliability of our simulations for the 2011–2014 period. On a national scale, the averaged CBO concentration is 42.7 ppbv, constituting 90% of the CTO (47.5 ppbv) in PD. The modeled ratio aligns well with previous studies using various models and methodologies, which have reported CBO contributions between 71% and 94% (Wang et al., 2011; Lu et al., 2019; Ye et al., 2024; Sahu et al., 2021). This spatial pattern of CBO largely resembles that of CTO, confirming that CBO is the dominant component of the ozone burden in most regions of China. In contrast, the CPO is relatively modest, averaging 4.8 ppbv nationwide. Building on the sensitivity simulations, the CBO is further decomposed into NBO (33.3 ppbv) and FPO (9.4 ppbv). NBO accounts for 78% of CBO, and its spatial pattern closely aligns with that of CBO, underscoring the key role of natural sources in ozone pollution in China. FPO is markedly elevated along the eastern coastline and the southwestern borders, clearly pinpointing transboundary transport as an important contributor to CBO (22%).

The spatial distribution and national averaged ratio of annual mean CBO to CTO is presented in Fig. 4. As the substantial emission reduction under SSP1-1.9, the ratio of CBO to CTO increases from 89.9% in PD to 91.2% in MC, while the ratio does not change under SSP5-8.5 (89.7%). The dominance of CBO is particularly evident in western China under SSP1-1.9, where anthropogenic precursor emissions are minimal. Despite the decrease in CTO under SSP1-1.9 and increase in CTO under SSP5-8.5 in mid-21st century relative to PD, the relative contribution of CBO remains consistently high, highlighting its critical role in shaping current and future ozone pollution in China.

Figure. 5 illustrates the changes in annual mean CTO and its major source

https://doi.org/10.5194/egusphere-2026-1839
Preprint. Discussion started: 7 September 2026

components in MC under the SSP1-1.9 and SSP5-8.5 scenarios relative to PD. Under the SSP1-1.9 scenario (Fig. 5a-e), CTO decreases across most of China except over the NCP, with a national mean reduction of 4.7 ppbv. The future ozone reduction under SSP1-1.9 is primarily driven by a 3.7 ppbv decline in CBO, which accounts for approximately 79% of the total change. The strong reductions occur over western and border regions, reflecting the effects of coordinated global mitigation efforts in suppressing background ozone levels. CPO also decreases by 1.1 ppbv, reflecting the impact of domestic precursor emission controls under the SSP1-1.9 scenario. Nevertheless, a regional increase in CPO is identified over NCP, causing the elevated level of CTO over this region. NBO exhibits a modest increase (+1.0 ppbv), associated with enhanced photochemical activity under a warmer climatic condition. Meanwhile, FPO declines more substantially (–4.7 ppbv), leading to an overall reduction in CBO. The decrease in FPO exceeds the climate-driven increase in NBO, reflecting the global benefits of coordinated emission mitigation strategies.

Under the SSP5-8.5 scenario (Fig. 5f-j), CTO exhibits a significant nationwide growth by 7.3 ppbv in MC relative to PD, with approximately 90% attributed to elevated CBO (6.5 ppbv). NBO is the dominant contributor to the increase in CBO, with a projected rise of 6.7 ppbv, indicating a substantial climate-driven enhancement in natural emissions in a much warmer future. FPO shows negligible change on the national scale (–0.2 ppbv), yet localized enhancements are observed over southwestern China, which contribute to the increased concentrations in that region. CPO exhibits a modest increase of 0.8 ppbv under SSP5-8.5, with relatively greater changes occurring in eastern China, contributing the CTO enhancement. These results indicate that, under a high-emission and unleashed-climate future, surface ozone increases in China will be primarily dominated by background sources.

To further elucidate the regional characteristics of future changes in background ozone under the diverse scenarios, we examine the seasonal mean near-surface ozone in China and its contributors under future emission and climate scenarios in Figs. 6–8. The absolute concentrations of different components in the PD and MC under the SSP119 and SSP585 scenarios are provided in Figs. S2–S4. Compared to the PD

https://doi.org/10.5194/egusphere-2026-1839
Preprint. Discussion started: 7 September 2026

condition, CTO under the SSP1-1.9 scenario shows a clear seasonal pattern, with the most pronounced reduction occurring in summer (–10.2 ppbv), followed by spring (–5.1 ppbv), autumn (–4.0 ppbv). The reduction in summer is largely driven by a substantial decrease in CPO, which declines by 6.9 ppbv, reflecting the effectiveness of stringent domestic emission controls implemented under the SSP1-1.9 sustainability scenario. In spring and autumn, the decline in CTO is primarily attributed to the reduction in CBO, which accounts for 92% and 83% of the decreases in CTO, respectively, with the most significant reductions occurring in western China and border regions. In winter, the nationally averaged CTO exhibits a slight increase of 0.3 ppbv, accompanied by pronounced spatial heterogeneity. The increase is most evident over the NCP, whereas most regions in western China show a decline. The enhanced CTO over the NCP is primarily attributed to a rise in CPO, likely resulting from weakened NO titration due to declining NO_x emissions, which facilitates ozone accumulation under VOC-limited conditions (Hou et al., 2023; Kang et al., 2025). A similar but weaker increase in ozone is also observed in spring and autumn over the NCP, which may be partly attributed to the potential bias inozone prediction under the low emission scenario in most global models (Ni et al., 2026). Nevertheless, it does not largely affect the focus of background ozone evaluation in this study.

The future changes in seasonal CBO can be further decomposed into the changes in NBO and FPO (Figs. 8a-h). The rise in NBO (0.5–1.5 ppbv) in MC under SSP1-1.9 relative to PD, mainly over eastern China, reflects strengthened ozone production from natural sources due to climate-driven increases in natural emissions (e.g., biogenic VOCs and soil NO_x emissions). In contrast, FPO decreases considerably in all seasons (–3.8 ~ –6.2 ppbv), especially over western China and border regions where the influence of transboundary transport is most evident, peaking in spring with strong westerly jets. As a result, the modest rise in NBO is offset by the substantial decline in FPO, leading to a net decrease in CBO under SSP1-1.9.

Under the SSP5-8.5 scenario, CTO shows a marked nationwide increase relative to PD, with seasonal enhancements ranging from 6.4 ppbv in winter to 8.1 ppbv in summer (Fig. 7). CBO is the dominant contributor to the increased CTO, constituting

https://doi.org/10.5194/egusphere-2026-1839
Preprint. Discussion started: 7 September 2026

87–91% of the total enhancement. The increase in CBO is particularly pronounced central and western China, suggesting that regions with limited anthropogenic emissions may face growing challenges from background ozone pollution in a much warmer future. The increase in ozone from domestic anthropogenic sources remains relatively small, ranging from +0.7 to +1.0 ppbv, with spatial increases mainly confined in urbanized eastern China.

The increase in CBO under SSP5-8.5 is primarily driven by the enhanced NBO (Fig. 8i–p), which exhibits a rise across the country, with national increases of 5.8–7.4 ppbv. This widespread growth in the NBO highlights that climate-sensitive precursors, including both increased natural emissions and rising CH_4 concentrations, have become the primary drivers of ozone increase under the strong warming scenario. The contribution of FPO shows insignificant changes, ranging from 0.1 to 0.4 ppbv, although localized increases are still showed in southwestern China, which further contribute to the increase in CBO. These findings suggest that under the SSP5-8.5, future ozone pollution in China will be increasingly dominated by natural sources, posing greater challenges for effective mitigation through domestic emission controls alone.

The vertical distribution of ozone provides insights into how its components respond differently to changes in climate and emissions at various altitudes. Figs. 9–11 compare vertical differences in ozone components between MC and PD under SSP1-1.9, SSP5-8.5, with a focus on eastern China (averaged over 110°E–122.5°E), a hotspot of human exposure to ozone pollution. Under the SSP1-1.9 scenario, the wintertime ozone increase in the lower troposphere is primarily due to a rise in CPO from domestic anthropogenic emissions near the surface (Fig. 9). This contrasts with the upper-level decreases driven by a reduction in CBO, which highlights the distinct vertical impacts of local chemical production versus long-range transport from foreign regions. A similar pattern of near-surface CTO increase is also evident over the NCP during spring and autumn. In summer, CTO decreases significantly by more than 10 ppbv from the surface to the middle of the troposphere, primarily due to the reduced CPO, which reflects the effectiveness of domestic emission controls under high photochemical

https://doi.org/10.5194/egusphere-2026-1839
Preprint. Discussion started: 7 September 2026

activity. The vertical extension of NBO increase implies a climate-related enhancement of natural precursor emissions that affects ozone throughout the lower troposphere (Fig. 11). However, the NBO increase does not suffice to offset the reduction in transboundary contributions. The concurrent increase in NBO and decrease in FPO further illustrates the interplay between climate-amplified natural source contributions and successful global coordination of emission controls, highlighting the dual challenges and co-benefits of integrated climate-air quality management.

In contrast to SSP1-1.9, the SSP5-8.5 scenario leads to widespread ozone increases over eastern China below the middle of the troposphere that are consistent across all seasons (Fig. 10). The pervasive vertical increase in CTO under SSP5-8.5 is primarily attributed to the enhanced CBO, signaling the growing dominance of background processes over local anthropogenic contributions. NBO exhibits a top-down enhancement pattern, with stronger increases in the mid-troposphere than near the surface, suggesting that downward transport from higher atmospheric layers may significantly contribute to the rise in background ozone.

5. Mechanistic drivers of the changing background ozone

As mentioned above, the future changes in CBO are controlled by transboundary transport related to the changes in foreign anthropogenic emissions under SSP1-1.9 and background sources in a warmer climate under SSP5-8.5. In this section, mechanistic drivers of the changing CBO are further illustrated by analyzing the future changes in anthropogenic emissions (Fig. 12), meteorological fields (Fig. S5) and the associated physical and chemical processes (Fig. 13).

Under SSP1-1.9, anthropogenic emissions show widespread and substantial reductions, with global annual emissions of NO_x, CO, and NMVOCs decreasing by 52.5 Tg yr^{-1} (−68%), 409.4 Tg yr^{-1} (−68%), and 88.2 Tg yr^{-1} (−74%) in MC relative to PD, respectively. Apart from China, regions such as South Asia, Southeast Asia, Europe, and North America also show considerable reductions, which collectively weaken the transboundary transport of ozone and precursor gases into China under the low emission scenario. Under the SSP5-8.5 scenario, changes in global anthropogenic precursor emissions are relatively modest. Significant increases of NO_x emissions are

https://doi.org/10.5194/egusphere-2026-1839
Preprint. Discussion started: 7 September 2026

also observed in South Asia, explaining the weak increase in FPO over southwestern China (Fig. 5j). CO emissions show an overall decline, with a smaller reduction compared to SSP1-1.9, and global NMVOC emissions decrease slightly by approximately 6.7 Tg yr^{-1}.

Changes in key meteorological factors in MC relative to PD show that under SSP1-1.9, surface temperature over eastern China increases by approximately 1 K, accompanied by enhanced surface shortwave radiation and reduced relative humidity. These changes promote higher photochemical reaction rates and stimulate more natural precursor emissions, driving an increase in net photochemical production of ozone by +52.5 Gg yr^{-1} in China. While changes in circulation-related meteorological parameters, such as wind patterns, are relatively modest, the significant reduction in anthropogenic precursor emissions from surrounding regions weakens the background ozone supply to China, leading to a substantial negative contribution from horizontal advection (−84.8 Gg yr^{-1}). This weakening of transboundary contribution (FPO) is consistent with the finding in Wang and Liao (2022), which reported a decrease of approximately 1.6 ppbv in the transport contribution from South and Southeast Asia to ozone over China between 2015 and 2050 under SSP1-1.9 with fixed climate conditions but varied anthropogenic emissions. Therefore, the decrease in CBO under SSP1-1.9 is primarily driven by large-scale reductions in global anthropogenic emissions and the associated weakening of transboundary influence, while enhanced chemical production under the favorable meteorological conditions partly offsets this effect.

Under SSP5-8.5, surface temperature undergoes sharp increases across China. However, in eastern China, where photochemical activity is most pronounced, anomalies in surface shortwave radiation and relative humidity are minor. Despite the modest response of several meteorological variables, temperature is widely recognized as a key meteorological driver modulating future ozone changes over China (Kang et al., 2025). In the context of stronger warming, the budget diagnosis reveals that the net chemical production increases by 70.6 Gg yr^{-1}, which indicates an enhancement in NBO and emerges as the dominant process driving the rise in CBO under SSP5-8.5. Horizontal advection contributes negatively (–38.4 Gg yr^{-1}), suggesting that transport

https://doi.org/10.5194/egusphere-2026-1839
Preprint. Discussion started: 7 September 2026

acts to weaken the rise in tropospheric background ozone, but the overall response remains dominated by chemical production. The process-based budget diagnostics are consistent with the sensitivity attribution, jointly indicating the future changes in CBO are dominated by the weakened foreign anthropogenic influence under SSP1-1.9 and enhanced climate-driven chemistry under SSP5-8.5.

In the simulations, future changes in CBO can also be affected by the time-varying CH_4 concentrations. To isolate the impact of CH_4, an additional set of simulations (NO_CH4low) with the CH_4 concentrations fixed at the pre-industrial level (1850 year) is conducted, yielding the pre-industrial natural background ozone (PNB). Compared to the PD level of 28.5 ppbv in China (Fig. S6), PNB rises by 2.6 and 3.8 ppbv under SSP1-1.9 and SSP5-8.5, respectively, indicating that climate change alone, even without future methane growth, can enhance CBO. Therefore, while controlling CH_4 remains essential for mitigating background ozone, climate adaptation strategies should also account for the persistent contribution from non-methane natural sources under warming conditions, including enhanced biogenic VOCs emissions, soil NO_x release, lightning activity, and stratosphere-to-troposphere exchange that contribute to elevated background ozone levels.

6. Conclusion and Discussion

Background ozone defines the baseline for regional pollution and the air quality improvements achievable through domestic emission controls, making its understanding crucial for informing ozone standards and guiding control strategies. In this study, future changes in near-surface ozone concentrations across China in mid-21st century (MC) under the SSP1-1.9 and SSP5-8.5 scenarios relative to the present-day (PD) condition are quantified based on GEOS-Chem model, focusing on the dominant role of background ozone and its evolving source composition. The analysis reveals that CBO remains a major contributor to ozone in China, accounting for about 90% of annual mean CTO in both present-day and future climate and emission status. The persistent dominance of background ozone points to the need for a strategic shift from local measures toward regional coordination, global cooperation, and climate mitigation, as the potential for further air quality improvements through local emission

https://doi.org/10.5194/egusphere-2026-1839
Preprint. Discussion started: 7 September 2026

controls alone is increasingly limited.

Under the SSP1-1.9 scenario, CTO decreases by 4.7 ppbv relative to the PD, driven by a 3.7 ppbv reduction in CBO (accounting for 79% of the total decline). The decrease in CBO can be further attributed to changes in the contributions from NBO and FPO. FPO declines significantly by 4.7 ppbv, reflecting the effective suppression of transboundary transport related to global emission reductions, which is the major factor driving the reduction in CBO. In contrast, NBO increases slightly by 1.0 ppbv, driven by enhanced photochemical production due to climate warming and increased shortwave radiation. The budget diagnostics identify the reduced horizontal transport (–84.8 Tg yr^{-1}) as the key mechanism driving CBO reduction, confirming that weakened transboundary transport from surrounding regions, because of global emission cuts, is the primary cause of the decline in CBO. These findings underscore the effectiveness of globally coordinated mitigation in reducing CBO, despite the climate-driven NBO increases. The seasonal CTO changes follow a consistent pattern across most regions and seasons, except for a modest winter increase in the NCP driven by the weakened NO_x titration.

Under the SSP5-8.5 scenario, CTO increases by 7.3 ppbv, with approximately 90% of this rise attributed to CBO, underscoring its continued dominance in driving ozone levels. Unlike the SSP1-1.9 scenario, the increase in CBO is primarily driven by a substantial rise in NBO (6.7 ppbv), reflecting the enhanced photochemistry and the significant contribution of climate-sensitive natural sources to ozone concentration under the intensified warming scenario. An increase in net photochemical production of 70.6 Tg yr^{-1} confirms the dominance of chemical processes. Under a high-emission, warming future, ozone pollution in China will be increasingly governed by natural sources, suggesting the requirement of integrated climate-air quality management in the future.

We also calculate the population-weighted CTO/CBO (Fig. S8 and Text S1) and changes in radiative forcing at the top of the atmosphere, which are more related to human health and climate change, respectively. Even under SSP1-1.9, the population-weighted CTO will increase, attributed to the increase in CPO over the densely

https://doi.org/10.5194/egusphere-2026-1839
Preprint. Discussion started: 7 September 2026

populated eastern China, highlighting the importance of coordinated regional mitigation. The population-weighted CTO and CBO rise sharply under SSP5-8.5, indicating that climate-driven growth can elevate population health risks. The overall decline in CBO under SSP1-1.9 produces a negative change in radiative forcing of −0.12 W m^{-2} over China, while the increase in CBO under SSP5-8.5 leads to a positive radiative forcing change of +0.11 W m^{-2}. Climate mitigation suppresses background ozone levels, creating a co-benefit that reinforces warming reduction, whereas unchecked warming drives ozone increases that exacerbate health risks and impose an additional burden on the climate system.

This study quantifies the contributions of anthropogenic and background sources to ozone levels through emission shutdown sensitivity experiments, offering a clear and interpretable framework for isolating source contributions under changing climate and emission scenarios. Although widely used in source attribution studies, the approcah may still be subject to uncertainties due to nonlinear interactions, particularly within the complex tropospheric chemistry. To evaluate the uncertainty, additional perturbation experiments are conducted with 20% and 80% reductions in domestic emissions. The results indicate that the nonlinear residual is approximately 0.5 ppbv (Fig. S9), which accounts for about 10% of the ozone response under the 100% reductions simulation. This suggests that the impact of nonlinear effects is relatively small, further confirming the robustness and reliability of the emission shutdown approach employed in this study. Future work could further explore source-specific and nonlinear responses under evolving climate and emission conditions using advanced attribution techniques such as tagged tracers. In addition, as climate warming continues and anthropogenic emissions decline, natural sources are expected to play an increasingly important role in modulating background ozone. These findings highlight the need to better quantify the contributions of individual natural sources to ozone changes, thereby supporting the development of climate-resilient and source-specific air quality management strategies.

https://doi.org/10.5194/egusphere-2026-1839
Preprint. Discussion started: 7 September 2026

Author contributions. YY designed the research; ML performed the simulations and analyzed the data. All authors including PW, KL and HL discussed the results and wrote the paper.

Financial support. This study was supported by the National Natural Science Foundation of China (grant 42475032) and Jiangsu Innovation and Entrepreneurship Team (grant JSSCTD202346).

Competing interests. At least one of the (co-)authors is a member of the editorial board of Atmospheric Chemistry and Physics.

Code and data availability. The observed surface ozone concentrations in 2014 are derived from the China Ministry of Ecology and Environment (https://quotsoft.net/air/). The monthly mean tropospheric ozone data from OMI–MLS are downloaded from https://acd-ext.gsfc.nasa.gov/Data_services/cloud_slice/new_data.html. The GEOS-Chem model is available at http://wiki.seas.harvard.edu/geos-chem/index.php/GEOS-Chem_14.2.3. The climate outputs from GCAP 2.0 can be downloaded from http://atmos.earth.rochester.edu/input/gc/ExtData/GCAP2/CMIP6/. Population density across China was obtained from the Gridded Population of the World version 4 (GPWv4) dataset (https://www.earthdata.nasa.gov/data/projects/gpw).

https://doi.org/10.5194/egusphere-2026-1839
Preprint. Discussion started: 7 September 2026

References

Ainsworth, E. A., Yendrek, C. R., Sitch, S., Collins, W. J., and Emberson, L. D.: The Effects of Tropospheric Ozone on Net Primary Productivity and Implications for Climate Change, Annu. Rev. Plant Biol., 63, 637–661, https://doi.org/10.1146/annurev-arplant-042110-103829, 2012.

Bey, I., Jacob, D. J., Yantosca, R. M., Logan, J. A., Field, B. D., Fiore, A. M., Li, Q., Liu, H. Y., Mickley, L. J., and Schultz, M. G.: Global modeling of tropospheric chemistry with assimilated meteorology: Model description and evaluation, J. Geophys. Res., 106, 23073–23095, https://doi.org/10.1029/2001JD000807, 2001.

Chen, C., Chen, W., Guo, L., Wu, Y., Duan, X., Wang, X., and Shao, M.: A comprehensive review of tropospheric background ozone: definitions, estimation methods, and meta-analysis of its spatiotemporal distribution in China, Atmos. Chem. Phys., 25, 15145–15169, https://doi.org/10.5194/acp-25-15145-2025, 2025.

Chen, W., Guenther, A. B., Shao, M., Yuan, B., Jia, S., Mao, J., Yan, F., Krishnan, P., and Wang, X.: Assessment of background ozone concentrations in China and implications for using region-specific volatile organic compounds emission abatement to mitigate air pollution, Environ. Pollut., 305, 119254, https://doi.org/10.1016/j.envpol.2022.119254, 2022.

Chen, Z., Liu, J., Cheng, X., Yang, M., and Shu, L.: Stratospheric influences on surface ozone increase during the COVID-19 lockdown over northern China, npj Clim. Atmos. Sci., 6, 76, https://doi.org/10.1038/s41612-023-00406-2, 2023.

Colombi, N. K., Jacob, D. J., Ye, X., Yantosca, R. M., Bates, K. H., Pendergrass, D. C., Yang, L. H., Li, K., and Liao, H.: Large and increasing stratospheric contribution to tropospheric ozone over East Asia, Atmos. Chem. Phys., 26, 2623–2633, https://doi.org/10.5194/acp-26-2623-2026, 2026.

David, L. M., Ravishankara, A. R., Brewer, J. F., Sauvage, B., Thouret, V., Venkataramani, S., and Sinha, V.: Tropospheric ozone over the Indian subcontinent from 2000 to 2015: Data set and simulation using GEOS-Chem chemical transport model, Atmos. Environ., 219, 117039, https://doi.org/10.1016/j.atmosenv.2019.117039, 2019.

Ding, D., Xing, J., Wang, S., Chang, X., and Hao, J.: Impacts of emissions and meteorological changes on China's ozone pollution in the warm seasons of 2013 and 2017, Front. Environ. Sci. Eng., 13, 76, https://doi.org/10.1007/s11783-019-1160-1, 2019.

Emberson, L.: Effects of ozone on agriculture, forests and grasslands, Phil. Trans. R.

https://doi.org/10.5194/egusphere-2026-1839
Preprint. Discussion started: 7 September 2026

Soc. A., 378, 2183, https://doi.org/10.1098/rsta.2019.0327, 2020.

Gong, C. and Liao, H.: A typical weather pattern for ozone pollution events in North China, Atmos. Chem. Phys., 19, 13725–13740, https://doi.org/10.5194/acp-19-13725-2019, 2019.

Guenther, A. B., Jiang, X., Heald, C. L., Sakulyanontvittaya, T., Duhl, T., Emmons, L. K., and Wang, X.: The Model of Emissions of Gases and Aerosols from Nature version 2.1 (MEGAN2.1): an extended and updated framework for modeling biogenic emissions, Geosci. Model Dev., 5, 1471–1492, https://doi.org/10.5194/gmd-5-1471-2012, 2012.

Hou, X., Wild, O., Zhu, B., and Lee, J.: Future tropospheric ozone budget and distribution over east Asia under a net-zero scenario, Atmos. Chem. Phys., 23, 15395–15411, https://doi.org/10.5194/acp-23-15395-2023, 2023.

Hu, W., Zhao, Y., Lu, N., Wang, X., Zheng, B., Henze, D. K., Zhang, L., Fu, T.-M., and Zhai, S.: Changing Responses of PM2.5 and Ozone to Source Emissions in the Yangtze River Delta Using the Adjoint Model, Environ. Sci. Technol., 58, 628–638, https://doi.org/10.1021/acs.est.3c05049, 2024.

Hudman, R. C., Moore, N. E., Mebust, A. K., Martin, R. V., Russell, A. R., Valin, L. C., and Cohen, R. C.: Steps towards a mechanistic model of global soil nitric oxide emissions: implementation and space based-constraints, Atmos. Chem. Phys., 12, 7779 – 7795, https://doi.org/10.5194/acp-12-7779-2012, 2012.

Jaffe, D. A., Cooper, O. R., Fiore, A. M., Henderson, B. H., Tonnesen, G. S., Russell, A. G., Henze, D. K., Langford, A. O., Lin, M., and Moore, T.: Scientific assessment of background ozone over the U.S.: Implications for air quality management, Elem. Sci. Anth., 6, 56, https://doi.org/10.1525/elementa.309, 2018.

Jaffe, D., Price, H., Parrish, D., Goldstein, A., and Harris, J.: Increasing background ozone during spring on the west coast of North America, Geophys. Res. Lett., 30, 163, https://doi.org/10.1029/2003GL017024, 2003.

Kang, L., Liao, H., Li, K., Yue, X., Yang, Y., and Wang, Y.: Effects of 2010 – 2045 climate change on ozone levels in China under a carbon neutrality scenario: key meteorological parameters and processes, Atmos. Chem. Phys., 25, 3603 – 3621, https://doi.org/10.5194/acp-25-3603-2025, 2025.

Li, S., Chen, L., Huang, G., Lin, J., Yan, Y., Ni, R., Huo, Y., Wang, J., Liu, M., Weng, H. and Wang, Y.: Retrieval of surface PM2.5 mass concentrations over North China using visibility measurements and GEOS-Chem simulations, Atmos. Environ., 222, 117121, https://doi.org/10.1016/j.atmosenv.2019.117121, 2020.

https://doi.org/10.5194/egusphere-2026-1839
Preprint. Discussion started: 7 September 2026

Lu, X., Zhang, L., Chen, Y., Zhou, M., Zheng, B., Li, K., Liu, Y., Lin, J., Fu, T.-M., and Zhang, Q.: Exploring 2016–2017 surface ozone pollution over China: source contributions and meteorological influences, Atmos. Chem. Phys., 19, 8339–8361, https://doi.org/10.5194/acp-19-8339-2019, 2019.

Lyu, X., Li, K., Guo, H., Morawska, L., Zhou, B., Zeren, Y., Jiang, F., Chen, C., Goldstein, A. H., Xu, X., Wang, T., Lu, X., Zhu, T., Querol, X., Chatani, S., Latif, M. T., Schuch, D., Sinha, V., Kumar, P., Mullins, B., Seguel, R., Shao, M., Xue, L., Wang, N., Chen, J., Gao, J., Chai, F., Simpson, I., Sinha, B., and Blake, D. R.: A synergistic ozone-climate control to address emerging ozone pollution challenges, One Earth, 6, 964–977, https://doi.org/10.1016/j.oneear.2023.07.004, 2023.

Ma, Z., Xu, J., Quan, W., Zhang, Z., Lin, W., and Xu, X.: Significant increase of surface ozone at a rural site, north of eastern China, Atmos. Chem. Phys., 16, 3969–3977, https://doi.org/10.5194/acp-16-3969-2016, 2016.

McLinden, C. A., Olsen, S. C., Hannegan, B., Wild, O., Prather, M. J., and Sundet, J.: Stratospheric ozone in 3-D models: A simple chemistry and the cross-tropopause flux, J. Geophys. Res., 105, 14653–14665, https://doi.org/10.1029/2000JD900124, 2000.

Meinshausen, M., Vogel, E., Nauels, A., Lorbacher, K., Meinshausen, N., Etheridge, D. M., Fraser, P. J., Montzka, S. A., Rayner, P. J., Trudinger, C. M., Krummel, P. B., Beyerle, U., Canadell, J. G., Daniel, J. S., Enting, I. G., Law, R. M., Lunder, C. R., O'Doherty, S., Prinn, R. G., Reimann, S., Rubino, M., Velders, G. J. M., Vollmer, M. K., Wang, R. H. J., and Weiss, R.: Historical greenhouse gas concentrations for climate modelling (CMIP6), Geosci. Model Dev., 10, 2057–2116, https://doi.org/10.5194/gmd-10-2057-2017, 2017.

Murray, L. T., Leibensperger, E. M., Orbe, C., Mickley, L. J., and Sulprizio, M.: GCAP 2.0: a global 3-D chemical-transport model framework for past, present, and future climate scenarios, Geosci. Model Dev., 14, 5789–5823, https://doi.org/10.5194/gmd-14-5789-2021, 2021.

Murray, L. T., Leibensperger, E. M., Mickley, L. J., and Tai, A. P. K.: Estimating future climate change impacts on human mortality and crop yields via air pollution, Proc. Natl. Acad. Sci. U.S.A., 121, e2400117121, https://doi.org/10.1073/pnas.2400117121, 2024.

Ni, R., Lin, J., Yan, Y., and Lin, W.: Foreign and domestic contributions to springtime ozone over China, Atmos. Chem. Phys., 18, 11447–11469, https://doi.org/10.5194/acp-18-11447-2018, 2018.

Ni, Y., Yang, Y., Wang, H., Wang, P., Li, K., Chen, L., Zhu, J., Li, B., and Liao, H.: Machine learning-based bias-corrected future projections of ozone concentrations from

https://doi.org/10.5194/egusphere-2026-1839
Preprint. Discussion started: 7 September 2026

a chemistry-climate model, Environ. Sci. Technol., 60, 3135 – 3147, https://doi.org/10.1021/acs.est.5c11992, 2026.

O'Neill, B. C., Kriegler, E., Riahi, K., Ebi, K. L., Hallegatte, S., Carter, T. R., Mathur, R., and Van Vuuren, D. P.: A new scenario framework for climate change research: the concept of shared socioeconomic pathways, Clim. Change, 122, 387–400, https://doi.org/10.1007/s10584-013-0905-2, 2014.

Ott, L. E., Pickering, K. E., Stenchikov, G. L., Allen, D. J., DeCaria, A. J., Ridley, B., Lin, R.-F., Lang, S., and Tao, W.-K.: Production of lightning NOx and its vertical distribution calculated from three-dimensional cloud-scale chemical transport model simulations, J. Geophys. Res., 115, D04301, https://doi.org/10.1029/2009JD011880, 2010.

Parrish, D. D., Lamarque, J.-F., Naik, V., Horowitz, L., Shindell, D. T., Staehelin, J., Derwent, R., Cooper, O. R., Tanimoto, H., Volz-Thomas, A., Gilge, S., Scheel, H.-E., Steinbacher, M., and Fröhlich, M.: Long-term changes in lower tropospheric baseline ozone concentrations: Comparing chemistry-climate models and observations at northern midlatitudes, J. Geophys. Res., 119, 5719–5736, https://doi.org/10.1002/2013JD021435, 2014.

Riahi, K., van Vuuren, D. P., Kriegler, E., Edmonds, J., O'Neill, B. C., Fujimori, S., Bauer, N., Calvin, K., Dellink, R., Fricko, O., Lutz, W., Popp, A., Cuaresma, J. C., Kc, S., Leimbach, M., Jiang, L., Kram, T., Rao, S., Emmerling, J., Ebi, K., Hasegawa, T., Havlik, P., Humpenöder, F., Da Silva, L. A., Smith, S., Stehfest, E., Bosetti, V., Eom, J., Gernaat, D., Masui, T., Rogelj, J., Strefler, J., Drouet, L., Krey, V., Luderer, G., Harmsen, M., Takahashi, K., Baumstark, L., Doelman, J. C., Kainuma, M., Klimont, Z., Marangoni, G., Lotze-Campen, H., Obersteiner, M., Tabeau, A., and Tavoni, M.: The Shared Socioeconomic Pathways and their energy, land use, and greenhouse gas emissions implications: An overview, Global Environ. Chang., 42, 153–168, https://doi.org/10.1016/j.gloenvcha.2016.05.009, 2017.

Sahu, S. K., Liu, S., Liu, S., Ding, D., and Xing, J.: Ozone pollution in China: Background and transboundary contributions to ozone concentration and related health effects across the country, Sci. Total Environ., 761, 144131, https://doi.org/10.1016/j.scitotenv.2020.144131, 2021.

Shah, V., Keller, C. A., Knowland, K. E., Christiansen, A., Hu, L., Wang, H., Lu, X., Alexander, B., and Jacob, D. J.: Particulate Nitrate Photolysis as a Possible Driver of Rising Tropospheric Ozone, Geophys. Res. Lett., 51, e2023GL107980, https://doi.org/10.1029/2023GL107980, 2024.

Skipper, T. N., Hu, Y., Odman, M. T., Henderson, B. H., Mathur, R., and Russell, A. G.: Estimating US background ozone using data fusion, Environ. Sci. Technol., 55, 4504-

https://doi.org/10.5194/egusphere-2026-1839
Preprint. Discussion started: 7 September 2026

4512, https://doi.org/10.1021/acs.est.0c08625, 2021.

Turnock, S. T., Wild, O., Dentener, F. J., Davila, Y., Emmons, L. K., Flemming, J., Folberth, G. A., Henze, D. K., Jonson, J. E., Keating, T. J., Kengo, S., Lin, M., Lund, M., Tilmes, S., and O'Connor, F. M.: The impact of future emission policies on tropospheric ozone using a parameterised approach, Atmos. Chem. Phys., 18, 8953–8978, https://doi.org/10.5194/acp-18-8953-2018, 2018.

Vazquez Santiago, J., Hata, H., Martinez-Noriega, E. J., and Inoue, K.: Ozone trends and their sensitivity in global megacities under the warming climate, Nat. Commun., 15, 10236, https://doi.org/10.1038/s41467-024-54490-w, 2024.

Wang, H., Jacob, D. J., Le Sager, P., Streets, D. G., Park, R. J., Gilliland, A. B., and Van Donkelaar, A.: Surface ozone background in the United States: Canadian and Mexican pollution influences, Atmos. Environ., 43, 1310–1319, https://doi.org/10.1016/j.atmosenv.2008.11.036, 2009.

Wang, Y. and Liao, H.: The impacts of transport from South and Southeast Asia on O3 concentrations in China from 2015 to 2050, Chinese Sci. B., 67, 2043–2059, https://doi.org/10.1360/TB-2021-0707, 2022 (in Chinese).

Wang, Y., Li, K., Chen, X., Yang, Z., Tang, M., Campos, P. M. D., Yang, Y., Yue, X., and Liao, H.: Revisiting the high tropospheric ozone over southern Africa: role of biomass burning and anthropogenic emissions, Atmos. Chem. Phys., 25, 4455–4475, https://doi.org/10.5194/acp-25-4455-2025, 2025.

Wang, Y. and Liao, H.: The impacts of transport from South and Southeast Asia on O3 concentrations in China from 2015 to 2050, Chin. Sci. Bull., 67, 2043 – 2059, https://doi.org/10.1360/TB-2021-0707, 2022.

Wang, Y., Liao, H., Chen, H., and Chen, L.: Future Projection of Mortality From Exposure to PM2.5 and O3 Under the Carbon Neutral Pathway: Roles of Changing Emissions and Population Aging, Geophys. Res. Lett., 50, e2023GL104838, https://doi.org/10.1029/2023GL104838, 2023.

Wang, Y., Zhang, Y., Hao, J., and Luo, M.: Seasonal and spatial variability of surface ozone over China: contributions from background and domestic pollution, Atmos. Chem. Phys., 11, 3511–3525, https://doi.org/10.5194/acp-11-3511-2011, 2011.

Wang, Z., Zhang, H., Shi, C., Ji, X., Zhu, Y., Xia, C., Sun, X., Zhang, M., Lin, X., Yan, S., Zhou, Y., Xing, C., Chen, Y., and Liu, C.: Vertical and spatial differences in ozone formation sensitivities under different ozone pollution levels in eastern Chinese cities, npj Clim. Atmos. Sci., 8, https://doi.org/10.1038/s41612-024-00855-3, 2025.

https://doi.org/10.5194/egusphere-2026-1839
Preprint. Discussion started: 7 September 2026

Xu, C., Mao, H., and Liao, H.: Future Ozone Changes and Their Impacts on Vegetation and Human Health in China Under the Shared Socio‐Economic Pathways, J. Geophys. Res., 129, e2023JD040086, https://doi.org/10.1029/2023JD040086, 2024.

Yan, Q., Wang, Y., Cheng, Y., and Li, J.: Summertime clean-background ozone concentrations derived from ozone precursor relationships are lower than previous estimates in the southeast United States, Environ. Sci. Technol., 55, 12852-12861, https://doi.org/10.1021/acs.est.1c03035, 2021.

Yang, Y., Li, M., Wang, H., Li, H., Wang, P., Li, K., Gao, M., and Liao, H.: ENSO modulation of summertime tropospheric ozone over China, Environ. Res. Lett., 17, 034020, https://doi.org/10.1088/1748-9326/ac54cd, 2022.

Ye, X., Zhang, L., Wang, X., Lu, X., Jiang, Z., Lu, N., Li, D., and Xu, J.: Spatial and temporal variations of surface background ozone in China analyzed with the grid-stretching capability of GEOS-Chem High Performance, Sci. Total Environ., 914, 169909, https://doi.org/10.1016/j.scitotenv.2024.169909, 2024.

Yin, H., Lu, X., Sun, Y., Li, K., Gao, M., Zheng, B., and Liu, C.: Unprecedented decline in summertime surface ozone over eastern China in 2020 comparably attributable to anthropogenic emission reductions and meteorology, Environ. Res. Lett., 16, 124069, https://doi.org/10.1088/1748-9326/ac3e22, 2021.

Zhai, S., Jacob, D. J., Franco, B., Clarisse, L., Coheur, P., Shah, V., Bates, K. H., Lin, H., Dang, R., Sulprizio, M. P., Huey, L. G., Moore, F. L., Jaffe, D. A., and Liao, H.: Transpacific transport of Asian peroxyacetyl nitrate (PAN) observed from Satellite: Implications for Ozone, Environ. Sci. Technol., 58, 9760–9769, https://doi.org/10.1021/acs.est.4c01980, 2024.

Zhao, J., Zhang, Y., Bie, S., Bilsback, K. R., Pierce, J. R., and Chen, Y.: Changes in global DMS production driven by increased CO2 levels and its impact on radiative forcing, npj Clim. Atmos. Sci., 7, 18, https://doi.org/10.1038/s41612-024-00563-y, 2024.

Zhou, X., Li, M., Huang, X., Liu, T., Zhang, H., Qi, X., Wang, Z., Qin, Y., Geng, G., Wang, J., Chi, X., and Ding, A.: Urban meteorology–chemistry coupling in compound heat–ozone extremes, Nat Cities, 2, 847–856, https://doi.org/10.1038/s44284-025-00302-1, 2025.

https://doi.org/10.5194/egusphere-2026-1839
Preprint. Discussion started: 7 September 2026

802 **Table 1.** Experimental design in this study.

Simulation	Emission settings	Ozone output
BASE	Full-chemistry simulation including all anthropogenic emissions and online natural emissions.	CTO
NO_CHN	Same as BASE, but with anthropogenic emissions of ozone precursors removed within China.	CBO; CTO − CBO = CPO
NO_ANT	Same as BASE, but with anthropogenic emissions of ozone precursors removed globally.	NBO; CBO − NBO = FPO
NO_CH_4low	Same as NO_ANT, but with CH_4 fixed at the year-1850 level.	PNB

803

https://doi.org/10.5194/egusphere-2026-1839
Preprint. Discussion started: 7 September 2026

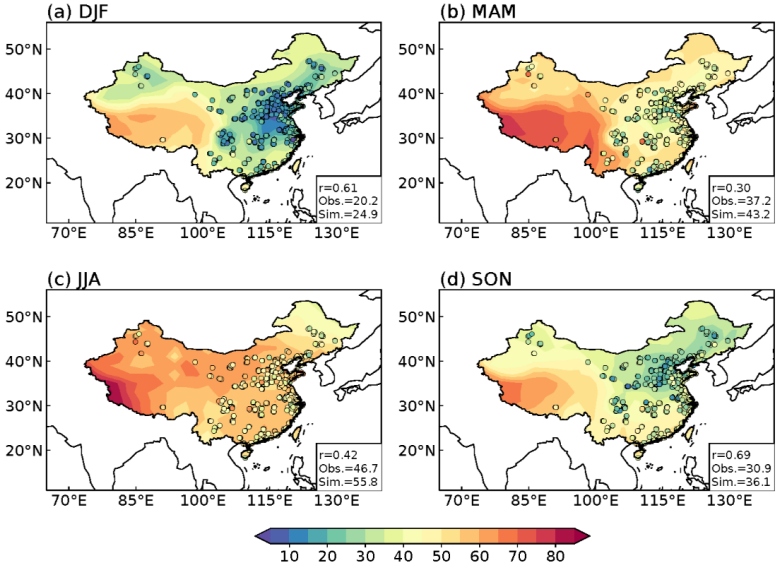

Figure 1. Spatial distribution of seasonal mean surface ozone concentrations (ppbv) over China in (a) winter (December-January-February, DJF), (b) spring (March-April-May, MAM), (c) summer (June-July-August, JJA), and (d) autumn (September-October-November, SON) in 2014 from GEOS-Chem simulation (colored background) and CNEMC observations (circles). Spatial correlation coefficients (r) between observed and simulated ozone concentrations and regional mean values from observation (Obs.) and simulation (Sim.) over the observational sites are indicated in bottom right of each panel.

https://doi.org/10.5194/egusphere-2026-1839
Preprint. Discussion started: 7 September 2026

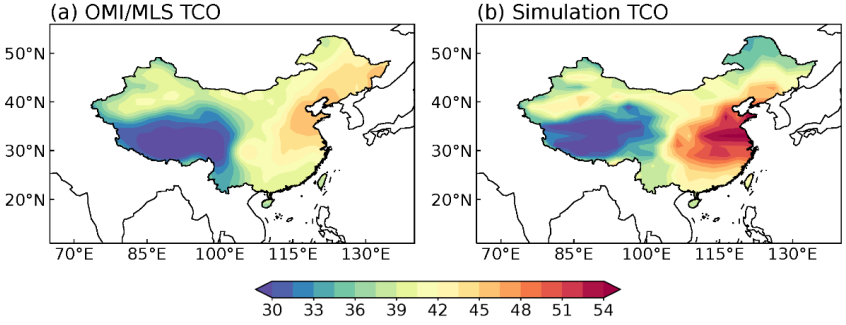

Figure 2. Spatial distribution of annual mean tropospheric column ozone (TCO, units: DU) over China during 2011–2014 based on (a) satellite retrievals from OMI/MLS and (b) GEOS-Chem BASE simulation.

https://doi.org/10.5194/egusphere-2026-1839
Preprint. Discussion started: 7 September 2026

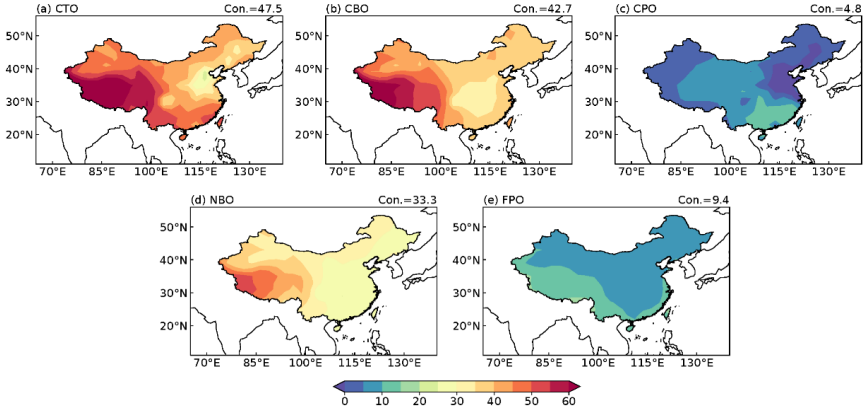

Figure 3. Spatial distributions of simulated annual mean concentrations (ppbv) of (a) China total ozone (CTO), (b) background ozone (CBO), (c) China pollution ozone (CPO), (d) natural background ozone (NBO), and (e) foreign pollution ozone (FPO) over China in PD. The regional mean value in China is shown in top right of each panel.

https://doi.org/10.5194/egusphere-2026-1839
Preprint. Discussion started: 7 September 2026

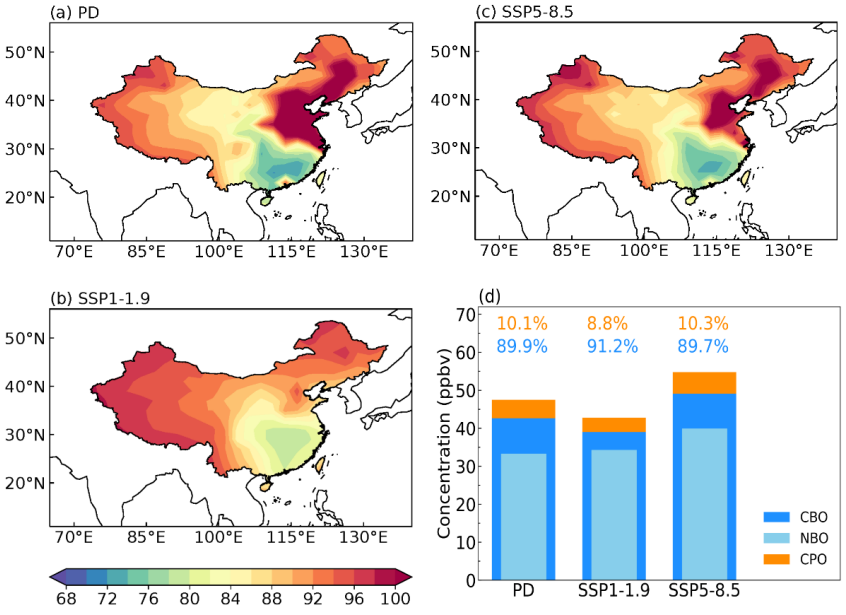

Figure 4. Spatial distributions of the background-to-total ozone ratio (CBO/CTO, %) in (a) PD and MC under (b) SSP1-1.9 and (c) SSP5-8.5 scenarios, and national average concentrations of CTO and its components (d). Bars represent CPO (orange), CBO (blue), and NBO (light blue) contributions. Percentages above bars indicate relative contributions of CPO and CBO to CTO.

https://doi.org/10.5194/egusphere-2026-1839
Preprint. Discussion started: 7 September 2026

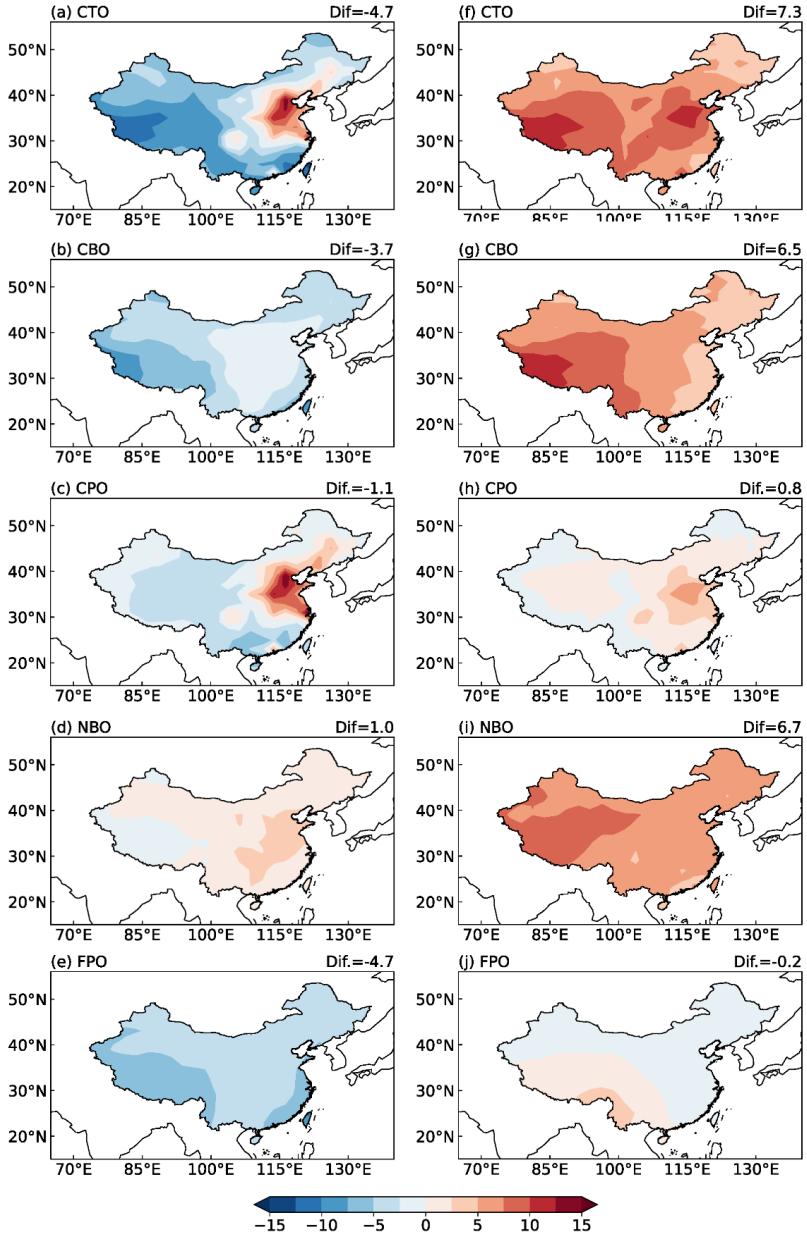

Figure 5. Spatial distributions of projected changes in annual mean surface ozone and its source components (CTO, CBO, CPO, NBO, and FPO) across China (Units: ppbv) in MC under (a–e) SSP1-1.9 and (f–j) SSP5-8.5 relative to PD. The value in the upper-right corner of each panel represents the regional mean in China.

https://doi.org/10.5194/egusphere-2026-1839
Preprint. Discussion started: 7 September 2026

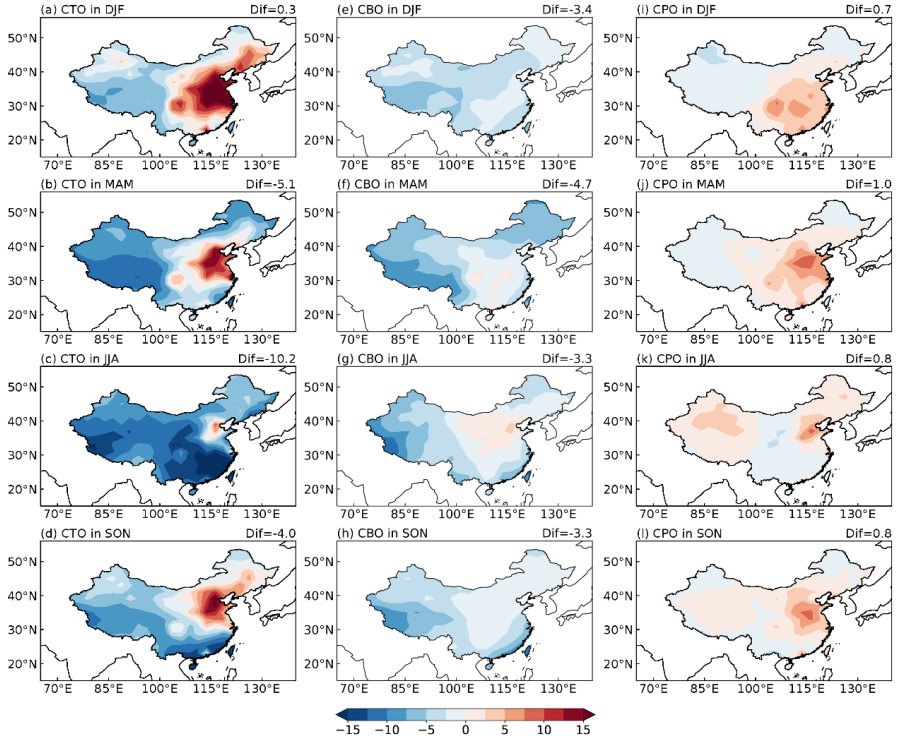

Figure 6. Spatial distribution of the differences in seasonal mean CTO, CBO, and CPO between MC under SSP1-1.9 and PD (Units: ppbv). The value in the upper-right corner of each panel represents the regional mean in China.

https://doi.org/10.5194/egusphere-2026-1839
Preprint. Discussion started: 7 September 2026

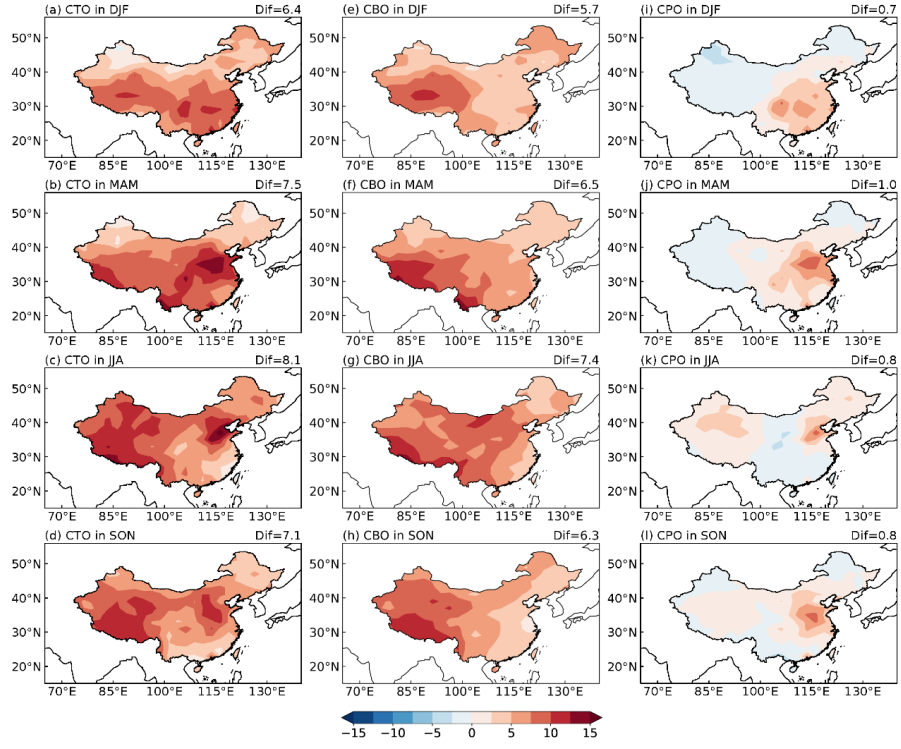

Figure 7. Spatial distribution of the differences in seasonal mean CTO, CBO, and CPO between MC under SSP5-8.5 and PD (Units: ppbv). The value in the upper-right corner of each panel represents the regional mean in China.

https://doi.org/10.5194/egusphere-2026-1839
Preprint. Discussion started: 7 September 2026

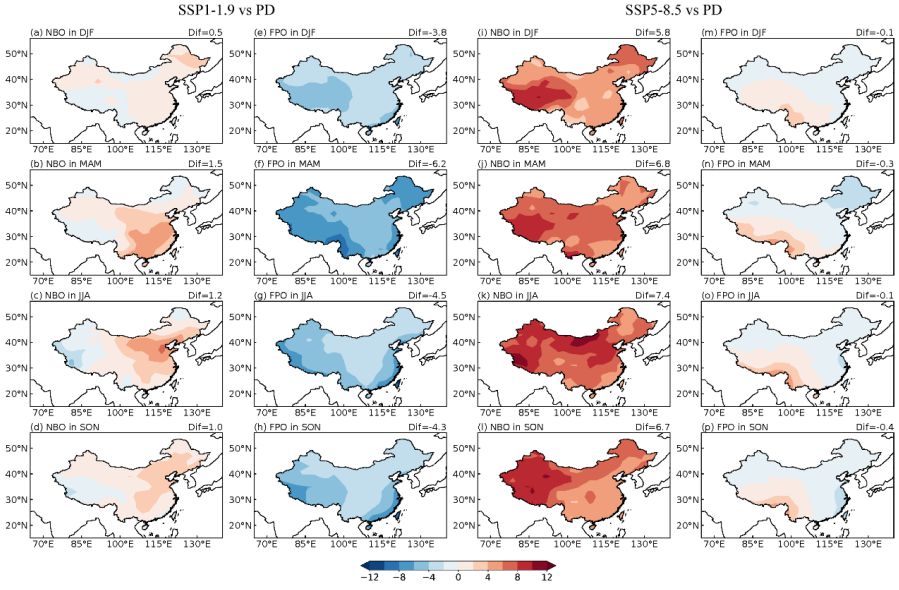

Figure 8. Spatial distribution of the differences in seasonal mean NBO and FPO between MC under SSP1-1.9 (a-h) and SSP5-8.5 (i-p) and PD (Units: ppbv). The value in the upper-right corner of each panel represents the regional mean in China.

https://doi.org/10.5194/egusphere-2026-1839
Preprint. Discussion started: 7 September 2026

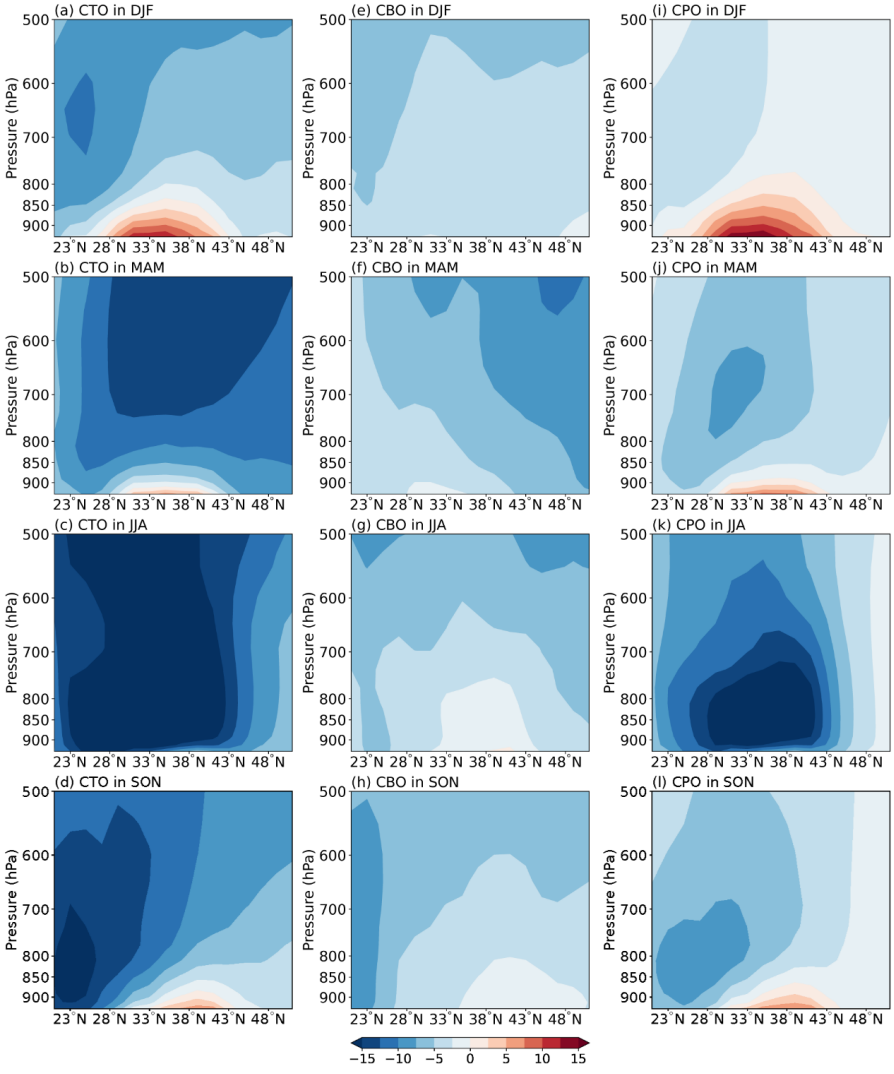

Figure 9. Pressure–latitude cross-section averaged over 110–122.5°E for differences in simulated seasonal mean CTO, CBO, and CPO between MC under SSP1-1.9 and PD (Units: ppbv).

https://doi.org/10.5194/egusphere-2026-1839
Preprint. Discussion started: 7 September 2026

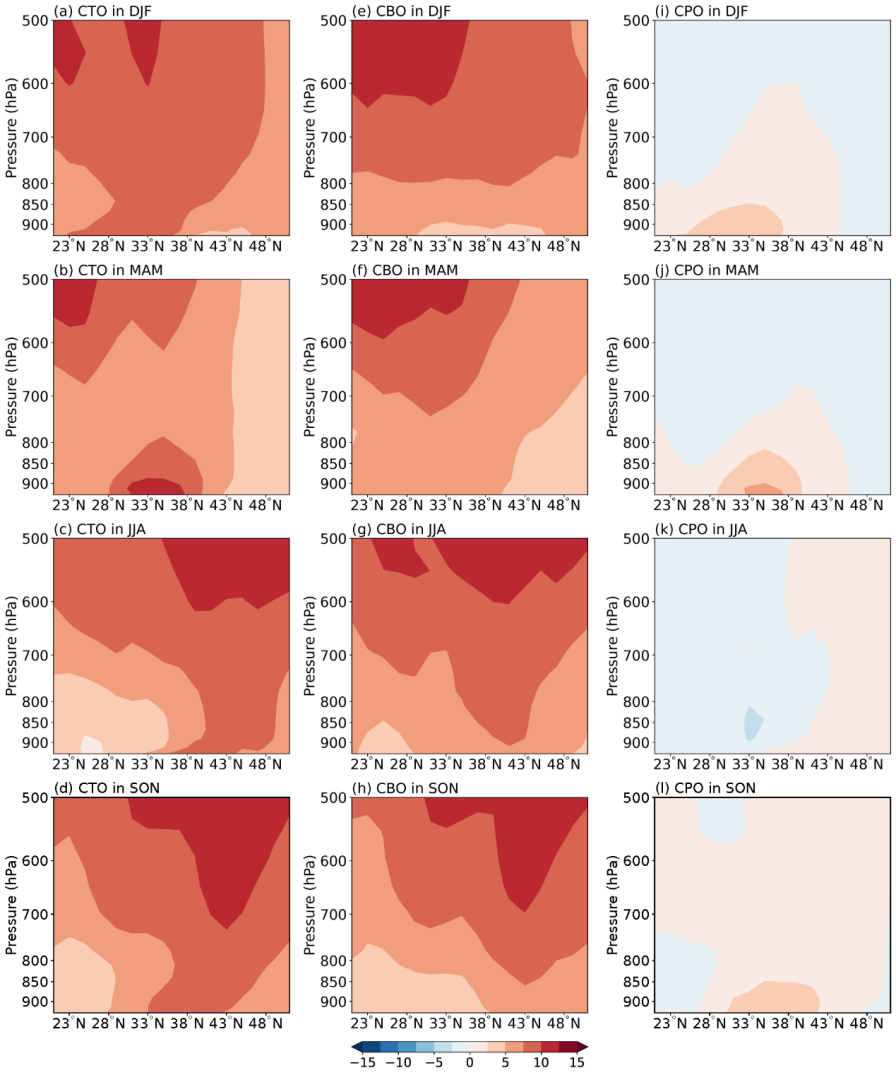

Figure 10. Pressure–latitude cross-section averaged over 110–122.5°E for differences in simulated seasonal mean CTO, CBO, and CPO between MC under SSP5-8.5 and PD (Units: ppbv).

https://doi.org/10.5194/egusphere-2026-1839
Preprint. Discussion started: 7 September 2026

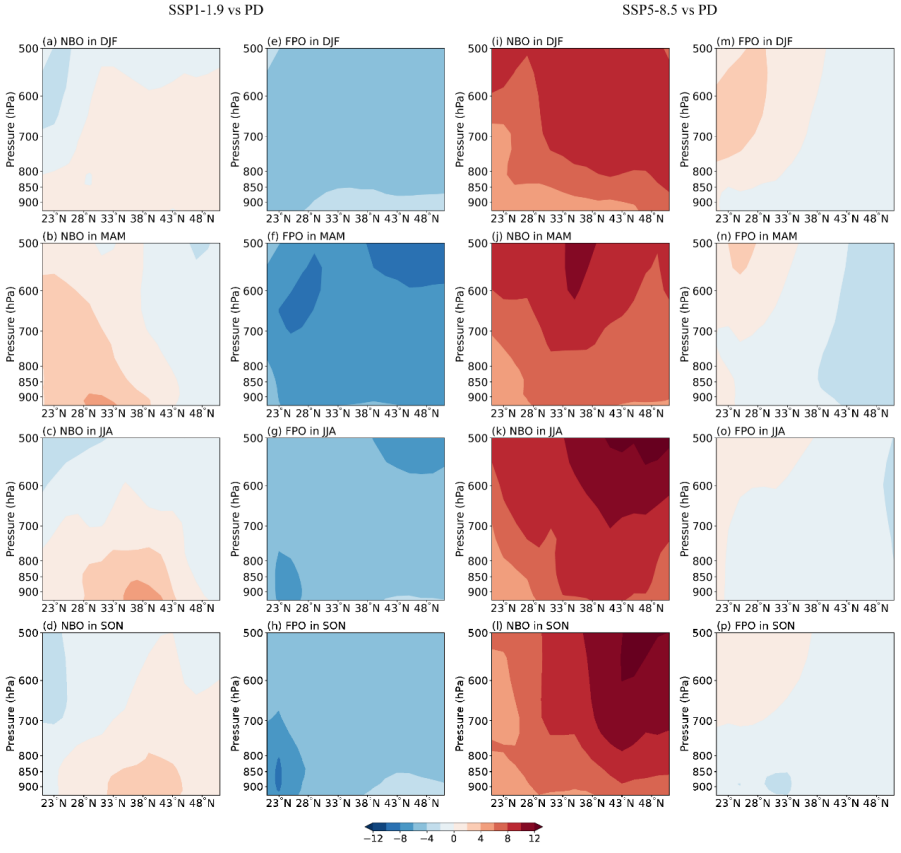

Figure 11. Pressure–latitude cross-section averaged over 110–122.5°E for differences in simulated seasonal mean NBO and FPO between MC under SSP1-1.9 and SSP5-8.5 and PD (Units: ppbv).

https://doi.org/10.5194/egusphere-2026-1839
Preprint. Discussion started: 7 September 2026

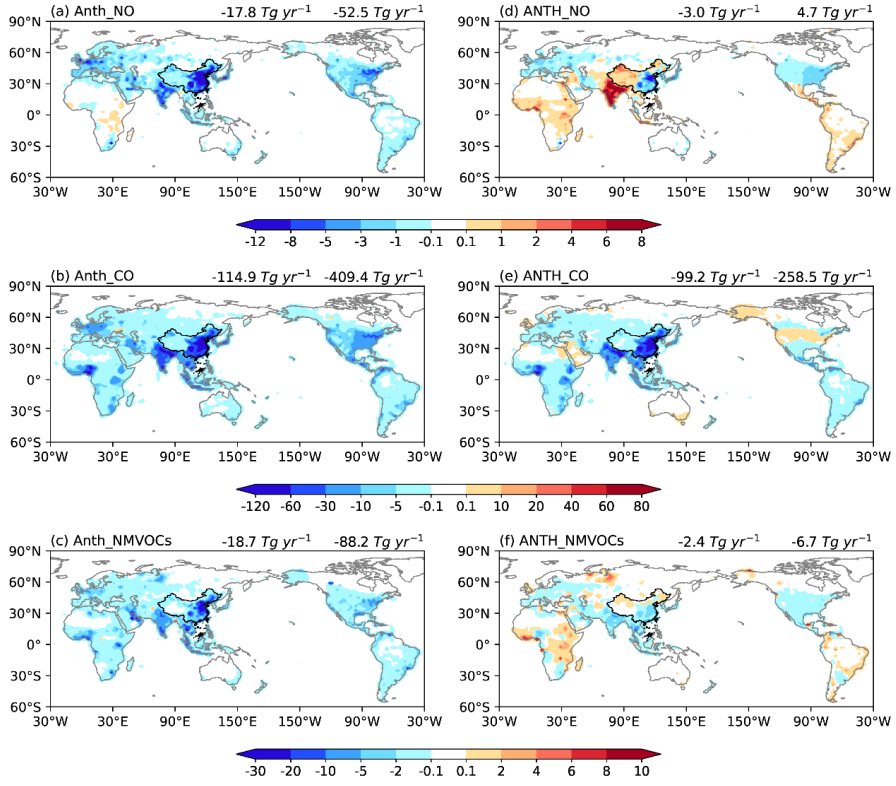

Figure 12. Spatial distribution of anthropogenic emission rates changes in (a) NO_x, (b) CO, and (c) NMVOCs in MC under the SSP1-1.9 (left) and SSP5-8.5 (right) scenarios relative to PD (Units: 10^{-11} kg m^{-2} s^{-1}). The values at the top of each panel are changes in annual total anthropogenic emissions for China and globe (Units: Tg yr^{-1}).

https://doi.org/10.5194/egusphere-2026-1839
Preprint. Discussion started: 7 September 2026

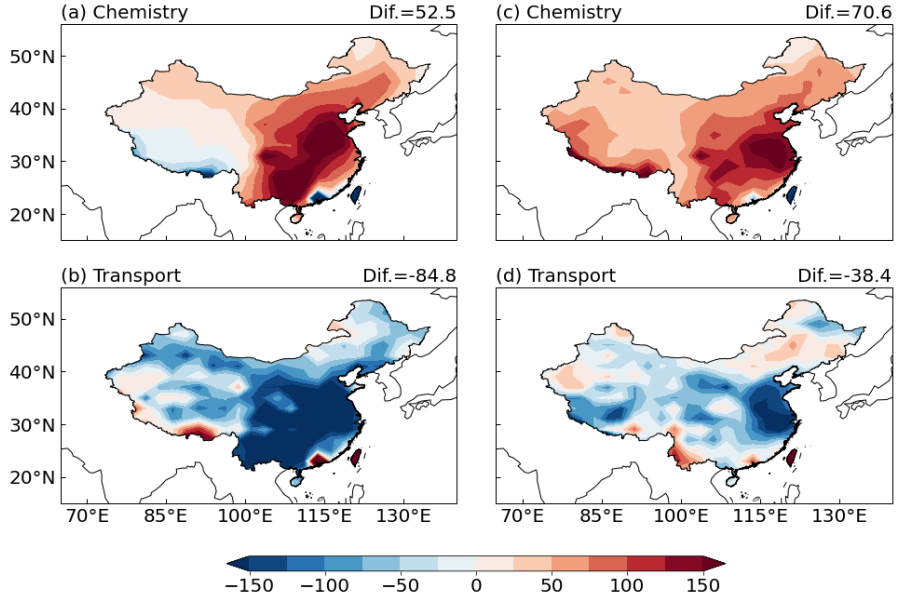

Figure 13. Spatial distribution of the difference in tropospheric ozone mass budgets of the (a, c) net chemical production (Chemistry), and (b, d) horizontal advection (Transport) between MC under SSP1-1.9 (left) and SSP5-8.5 (right) relative to PD. These results are derived from the NO_CHN experiments. The value in the upper-right corner of each panel represents the regional mean in China (units: Gg yr^{-1}).